

Propagation Measurements With Regional Train at 60 GHz for Virtual Coupling Application

Kun Yang¹, Marion Berbineau¹, Jean-Pierre Ghys¹, Yann Cocheril¹, Divitha Seetharamdoo¹,

¹Univ. Lille Nord de France, IFSTTAR, COSYS, LEOST, F-59650 Villeneuve d'scq,

20, rue Élisée Reclus - BP 70317, F-59666 Villeneuve d'Ascq

Email: kun.yang@ifsttar.fr

Abstract—A millimeter-wave (mmW) radio channel measurement campaign at 64.5 GHz for train's virtual coupling application was performed in a regional train in France. In this paper, we give a brief description of the channel sounder design and channel measurement campaigns with four dedicated scenarios including different setups and other channel parameters. The results of angular power distribution obtained by sweeping a horn antenna at the receiver side shows that the difference of the received signal levels (RSL) obtained at different azimuth angle of the same location can vary from 5 dB to 12 dB depending on different scenarios. Most of highest RSL are received at the angle of 0 degree. The mean delay and RMS delay spread have also been studied, from which it can be found that these parameters are uncorrelated with the TX-RX distance for the O2O and R2R scenarios while these parameter values turn out to be large for the O2D and O2DC scenarios at large TX-RX distances.

Index Terms—mmW, Angular power distribution, mean delay, RMS delay spread, virtual coupling.

I. INTRODUCTION

Today, more flexible use of trains in line is a strong need to allow more flexible accommodation of the capacity of the railway line at peak hour. To fulfill the requirements, automatic coupling of trains while they are moving is mandatory and rely on so called train's virtual coupling function. As explained in [1], virtual coupling aims to enable "virtually-coupled trains" to operate much closer to one another (within their absolute braking distance) and dynamically modify their own composition on the move (virtual coupling/uncoupling of train convoys), with at least the same level of safety as what is currently provided. Similar to platooning concept in the automotive domain, the preceding train and the adjacent train will be linked together by radio links to create a virtual coupling, running the trains together.

Consequently, this important innovative function has become an important bottleneck in terms of performance from the telecommunications point of view not only in terms of throughputs, latency, network dynamics and availability but also to guaranty the safety and security performances required for railway operation [2].

In a first step, the train's on-board Ethernet backbones should be connected without any physical connection but the trains are still mechanically coupled. Thus, trains manufactured by different companies and with different interfaces could be virtually coupled, driven together by the leading cabin and sharing the same traffic slot. Pushing

the concept to its limit, it would be possible to couple and uncouple consists on-the-fly (*i.e.* while both consists moving or even cruising) and increase significantly the capacity of the line by making long chains of virtually coupled trains. This can increase railway line capacity with more than 100%, possibly 300% [1].

Today, the radio system which is able to answer all the needs for train's virtual coupling is not yet defined. In [2] the author present a very interesting road map regarding the development of this function. Different solutions can be envisaged: direct radio communications, communication through external communication network or through the dedicated railway network, depending on which radio systems can fulfill the requirements.

The 60 GHz band was investigated more than 20 years ago for V2I communications in the context of automotive applications [3]. Today frequency bands above 10 GHz are investigated for very high throughputs applications in the context of 5G [4]. Frequency bands above 30 GHz are foreseen for various applications in the Railway context [5]. The 90 GHz band has been investigated recently for railway applications [7]. In this context, we consider that 60 GHz systems are very good candidates to fulfill the requirements for virtual coupling of trains. For this reason, in the context of the European project Roll2rail [6] we have investigated the radio channel at 60 GHz for Virtual coupling applications. The measurement campaign was performed at ALSTOM's premises near Valenciennes in France and we have considered Regional trains.

The rest of paper is organized as follows: in section II the radio channel sounder is described briefly. In section III the measurement campaign is presented in detail. Section IV is devoted to the analysis of the angular power distribution for four scenarios. Section V addresses the mean delay and RMS delay spread. Finally, conclusions are drawn in section VI.

II. THE CHANNEL SOUNDER

In order to measure the radio channel on train, we have built a radio channel measurement solution based on arbitrary wave generator (AWG), Tektronix Scope and mmW RF module designed by Vμbiq, which are listed in Table I:

The channel sounder (shown in Fig. 1(a)) consists of a transmitter sending a known chirp signal, and a receiver which

TABLE I
CHANNEL SOUNDER COMPONENTS

equipment	frequency	Bandwidth or sampling rate
V _μ biq mmW RF module	64.5 GHz	Up to 1.2 GHz
Tektronix Scope TDS6124	12 GHz	40 Gs
mmW antenna		60 GHz
Tektronix AWG 7102		10 GSs

analyzes the received signal, and stores information to files. The supported bandwidth is up to 1.2 GHz, while RF modules are configured to be operated at 64.5 GHz. The maximum measurable delay is $1.33 \mu\text{s}$. The transmitter and the receiver are synchronized by using a marker setting through a RF cable (up to 50 m). The channel sounder is modular and flexible, and can easily be configured for different measurement scenarios. Two identical horn antennas with a 15 dBi gain (see Fig. 1(b)) are utilized in the sounder system. The antenna beam width is 22 degrees, which is set as the sweep step of the motion controller.

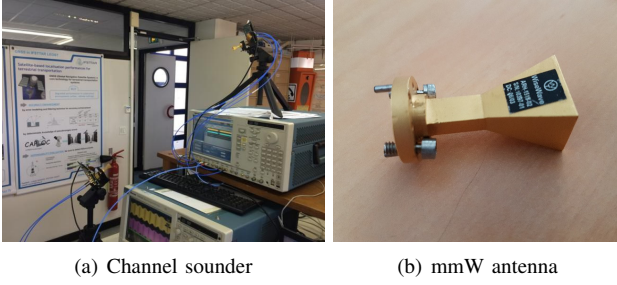


Fig. 1. channel sounder and antenna

The transmitter (TX) keeps on sending the chirp signal continuously. 14 consecutive chirps are recorded every time through the GPIB port introduced by Tektronix. Each chirp duration time is $1.33 \mu\text{s}$, which is corresponding to the maximum measurable delay.

III. THE MEASUREMENT CAMPAIGNS

The mmW radio technology is normally usable for the short-range radio link due to the high propagation loss. Besides, the mmW sounder system with integrated antennas is fragile. However, the possible high throughput can be achieved by the mmW radio technology due to large available bandwidth. By taking the feasibility into consideration, our measurement campaigns will be dedicated to short-distances (maximum 25 m) with limited mobility. In this paper, we focus on the mmW radio communication for the Virtual Coupling application. As a result, the following four scenarios are designed.

- 1) *Outdoor-to-Driver (O2D)*: in this scenario, the transmitter antenna is mounted inside the driver's cabin, while the Receiver is installed outside with the equivalent antenna height. The receiver takes several positions outside the cabin along the line shown in Fig. 2(a). Both TX and RX antenna height are 2.6 m. 7 RX locations are

considered with a location spacing of 3 m. The distance from every location to the side-line of the trail is 0.4 m. The distance from the first location to the TX is set to be 5 m. The RX antenna is swept between $[-22^\circ, +22^\circ]$ since the vibration of the train during the trip won't be more than this range. Here, 0° corresponds to the facing direction to the TX.

- 2) *Outdoor-to-Driver center (O2DC)*: similar with the O2D, this scenario is designed for the virtual coupling, in which the transmitter is located inside the driver cabin. The only difference between the O2DC and the O2D is that the RX is located in the middle of the track (see Fig. 2(b)). Similarly, both TX and RX antenna height are 2.6 m. 7 RX locations are designed with a location spacing of 3 m. The distance from the first location to the TX is set to be 5 m. The RX antenna is swept between $[-22^\circ, +22^\circ]$.
- 3) *Outdoor-to-Outdoor (O2O)*: in this scenario, the TX and the RX are mounted outside the train near the mechanical coupling system (see photography on Fig. 2(g)) in order to simulate a future transmission in the context of virtual coupling. The receiver is located at several positions on the same longitudinal axis as indicated on the scheme Fig. 2(c). Both TX and RX antenna height are 1.14 m. 7 RX locations are considered with a location spacing of 3m. The distance from location to the side-line of the trail is 0.4 m. The distance between the first location to the TX is set to be 4m. The RX antenna is swept between $[-22^\circ, +22^\circ]$.
- 4) *Roof-to-Roof (R2R)*: in this scenario, the transmitter is located on the roof of the train while the receiver is situated at the same height to simulate the virtual coupling when both TX and RX antenna are installed on the roof of the two trains. The transmitter is located on the roof of the train as illustrated on the photography given on Fig. 2(h). The receiver is situated on the ground and takes different positions as shown on the scheme given in Fig. 2(d). Both TX and RX antenna height are 4.5 m. The azimuth angles at the RX antenna were swept in 22° steps from -22° to $+22^\circ$, while the TX antenna is fixed on the roof the train.

Thanks to ALSTOM, we had access to Regional trains in Alstom' factory in Valenciennes in a garage. The measurement campaigns for the above scenarios are performed based on the available conditions. It needs to be mentioned that in our measurement campaign, there is only one train in the garage which can be used. However, these measurements still provide good information on the radio channel characteristics for the virtual coupling application. At the RX, a precise angular positioner is used to swept the RX antenna at different Azimuth angles, while a fix antenna angle is used at the TX side.

The main channel measurement parameters is summarized in Table II.

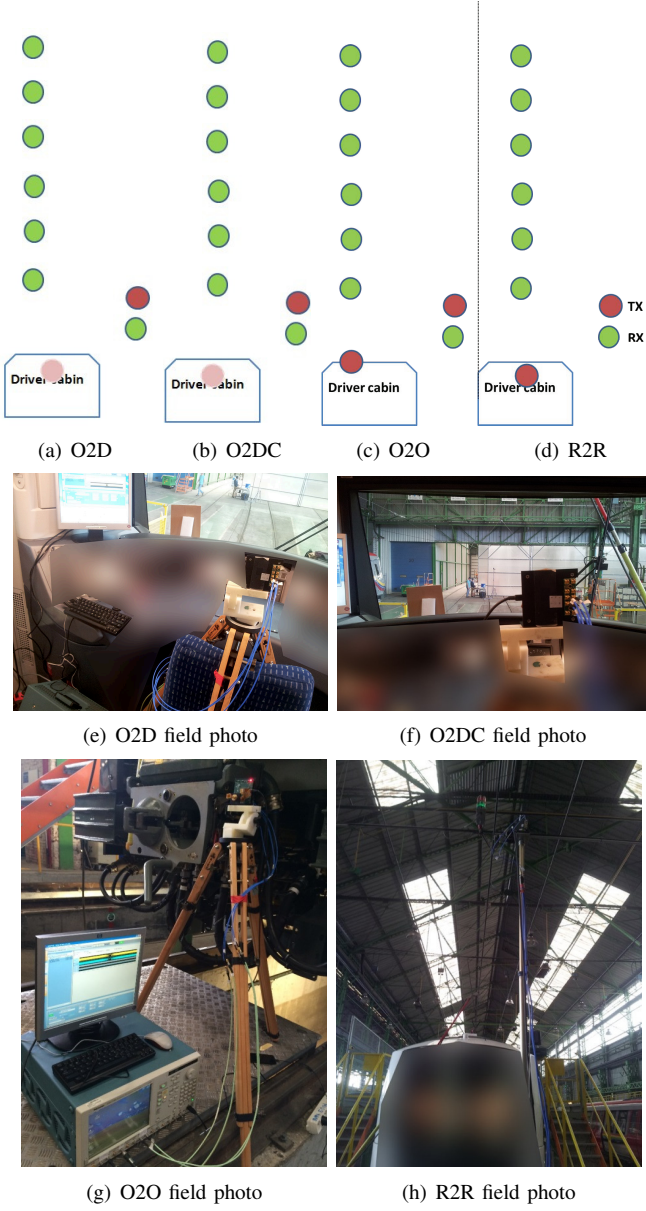


Fig. 2. Measurement scenarios and field test photos

TABLE II
CHANNEL MEASUREMENT PARAMETERS

Scenarios	O2D/O2DC	O2O	R2R
TX/RX ANT height	2.6 m	1.14 m	4.5
Swept AZ. angle	$[-22^\circ, +22^\circ]$	$[-22^\circ, +22^\circ]$	$[-22^\circ, +22^\circ]$
Location spacing	3m	3m	3m
First location distance	5m	4m	4m

IV. ANGULAR POWER DISTRIBUTION

In real operation, the train will vibrate during the moving, which will influence the radio channel for the virtual coupling application. Therefore, it is crucial to investigate the radio channel by taking the train vibration into consideration. However, the mmW horn antenna radiating pattern is not wide

enough to measure such kind of channel and it is important to sweep the mmW horn antenna at different azimuth angles. In our measurement campaign, the mmW antenna is swept in 22° steps from -22° to $+22^\circ$, which can cover classical train vibration range. From the measurement data, the angular power distribution is extracted for different scenarios, which is shown in the Fig. 3-6.

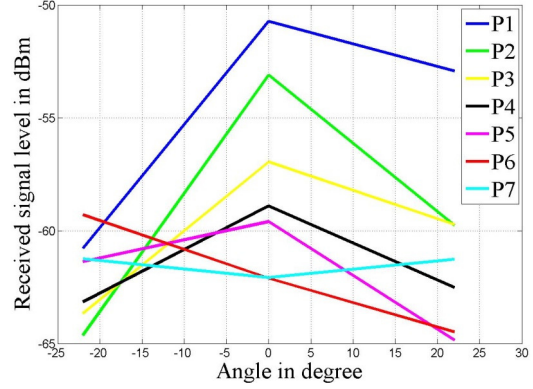


Fig. 3. Angular power distribution for the O2D scenario

Fig. 3 shows that from position P1 to P5 (up to 17 m), the highest received signal level (RSL) is obtained at the angle of 0 degree. When the TX-RX distance is more than 17 m (at position P6 and P7), the highest RSLs are received at the angle of -22° . However, the difference between the largest RSL and the smallest RSL is within 12 dB at the same location.

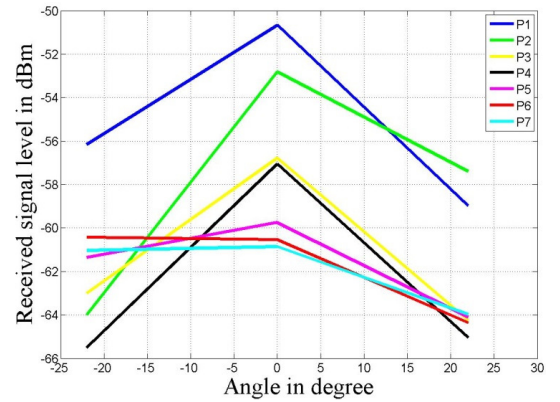


Fig. 4. Angular power distribution for the O2DC scenario

Fig. 4 shows that the highest RSLs are all received at the angle of 0 degree. The difference between the largest RSL and the smallest RSL is also within 12 dB at the same location.

Fig. 5 highlights that most of the peak RSLs (except at position P4) are received at the angle of 0 degree. The difference between the largest RSL and the smallest RSL is within 5 dB.

Fig. 6 shows that the highest RSLs are received at the angles of 0 degree and 22 degrees. The difference between the largest RSL and the smallest RSL is within 4 dB, which is ignorable.

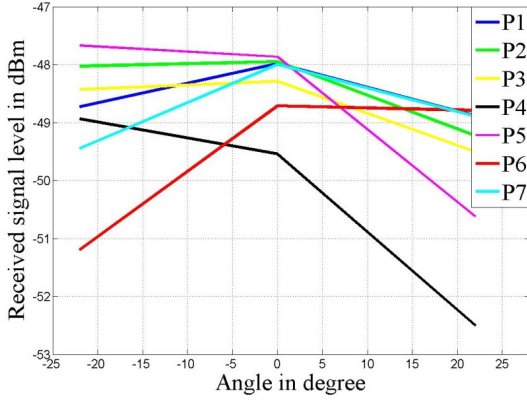


Fig. 5. Angular power distribution for the O2O scenario

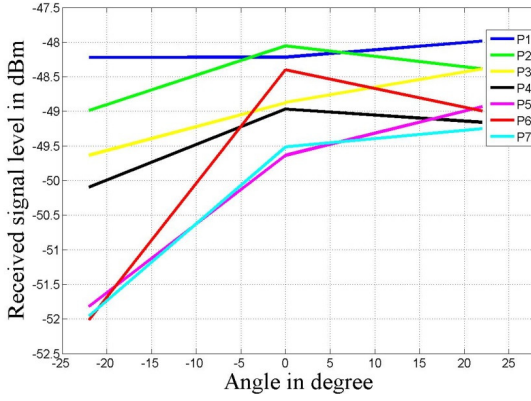


Fig. 6. Angular power distribution for the R2R scenario

It can be concluded that a dedicated antenna radiating pattern pointing to the TX is efficient for the O2D and O2DC scenarios, which can provide more than 10 dB gain. Even though the RSL difference for both the O2O and R2R scenarios is within 5 dB. This conclusion can also give some hints for the antenna design.

V. THE MEAN DELAY AND RMS DELAY SPREAD

During our measurement campaign, the bandwidth of 1.2 GHz is utilized, which leads to high resolution in the delay domain. The channel turns out to be frequency-selective by taking the structure of the train and the factory into consideration. Therefore, it is important to study the mean delay and the RMS delay spread, since both of them are regarded as important factors for the design of radio communication links. Besides, the system performance degradation due to inter-symbol interference (ISI) is correlated with them, which can provide information for a common rule of thumb in a communication system design [8] and channel equalization. As a result, it is necessary to study the mean excess delay and the RMS delay spread, which are expressed by using equation (1) and (2), respectively.

$$T_m = \frac{\int_{-\infty}^{\infty} P(\tau)\tau d\tau}{\int_{-\infty}^{\infty} P(\tau)d\tau} \quad (1)$$

TABLE III
MEAN DELAY (NS) VERSUS ANGLE POSITION FOR THE O2D SCENARIO

Degree	-22°	0°	+22°
P_1	8.6	8.5	8.4
P_2	7.6	8.2	7.7
P_3	15.8	7.7	7.7
P_4	9.7	7.6	7.7
P_5	501.6	8.4	8.0
P_6	555.9	7.1	7.3
P_7	467.8	8.4	16.5

TABLE IV
RMS DELAY SPREAD (NS) VERSUS ANGLE POSITION FOR THE O2D SCENARIO

Degree	-22°	0°	+22°
P_1	1.1	1.0	1.0
P_2	1.4	1.3	1.2
P_3	60.6	0.8	1.1
P_4	19.8	1.3	1.1
P_5	431.4	1.1	1.1
P_6	424.2	1.1	1.0
P_7	451.5	1.2	14.2

TABLE V
MEAN DELAY (NS) VERSUS ANGLE POSITION FOR THE O2DC SCENARIO

Degree	-22°	0°	+22°
P_1	6.6	6.8	6.8
P_2	7.0	6.9	6.9
P_3	7.1	7.1	6.5
P_4	7.3	7.1	7.1
P_5	410.9	7.7	7.8
P_6	402.6	8.0	7.6
P_7	297.8	7.8	7.8

TABLE VI
RMS DELAY SPREAD (NS) VERSUS ANGLE POSITION FOR THE O2DC SCENARIO

Degree	-22°	0°	+22°
P_1	0.9	1.0	1.3
P_2	1.3	1.6	0.9
P_3	1.7	1.3	1.5
P_4	1.2	1.1	0.8
P_5	451.7	0.9	0.8
P_6	470.3	1.0	0.9
P_7	424.5	1.3	1.5

$$S_\tau = \sqrt{\frac{\int_{-\infty}^{\infty} P(\tau)\tau^2 d\tau}{\int_{-\infty}^{\infty} P(\tau)d\tau}} - T_m^2 \quad (2)$$

where $P(\tau)$ represents the averaged PDP for each WSS region and τ is the delay of the delay path.

Tables III and IV illustrate that the RMS delay spread and the Mean delay at large TX-RX distance (Position P5, P6 and P7) are much larger at the angle of 22°, which means the existence of important reflections from surrounds that are incident at these setups.

Tables V and VI show that the RMS delay spread and the Mean delay at large TX-RX distance (Position P5, P6 and P7)

TABLE VII
MEAN DELAY (NS) VERSUS ANGLE POSITION FOR THE O2O SCENARIO

Degree	-22°	0°	+22°
P_1	7.8	7.9	7.9
P_2	7.9	8.1	7.9
P_3	8.5	8.5	8.3
P_4	9.2	9.4	8.9
P_5	7.2	7.1	7.1
P_6	8.6	8.2	8.1
P_7	8.3	8.3	8.7

TABLE VIII
RMS DELAY SREAD (NS) VERSUS ANGLE POSITION FOR THE O2O SCENARIO

Degree	-22°	0°	+22°
P_1	1.2	1.2	1.1
P_2	1.0	1.1	1.4
P_3	0.8	1.2	1.3
P_4	1.2	1.3	0.7
P_5	0.8	1.3	1.3
P_6	1.5	1.0	0.7
P_7	1.4	1.0	1.4

TABLE IX
MEAN DELAY (NS) VERSUS ANGLE POSITION FOR THE R2R SCENARIO

Degree	-22°	0°	+22°
P_1	8.4	8.5	8.5
P_2	7.1	7.2	7.0
P_3	7.1	7.3	7.4
P_4	8.1	8.4	8.4
P_5	6.8	6.7	7.1
P_6	8.2	8.4	8.1
P_7	8.5	8.7	8.6

TABLE X
RMS DELAY SREAD (NS) VERSUS ANGLE POSITION FOR THE R2R SCENARIO

Degree	-22°	0°	+22°
P_1	1.0	1.4	1.1
P_2	1.0	1.0	1.1
P_3	1.0	1.0	1.3
P_4	1.2	1.4	1.3
P_5	1.0	1.1	1.4
P_6	1.0	1.0	1.2
P_7	1.3	1.2	1.5

are much larger at the angle of 22°, which is consistent with the results obtained for O2D scenario.

Tables VII and VIII highlight that the RMS delay spread and the Mean delay are small and consistent, which shows that the RMS delay spread and the Mean delay are uncorrelated with the TX-RX distance. It can also be concluded that few reflections from the environment are experienced.

Similar with the O2O scenario, it can be found in Tables IX and X that the RMS delay and the Mean delay are small and consistent, which shows that the RMS delay and the Mean delay are uncorrelated with the TX-RX distance. It can also be concluded that few reflections from O2O and R2R environments exist.

VI. CONCLUSIONS

A channel measurement campaign at 64.5 GHz has been carried out for regional train environments in France at Alstom's premise. The RX horn antenna was swept by using a precise motion controller to investigate Angular power distribution. The channel sounder, measurement set-up, environments, antenna characteristics and parameters have been described briefly. The difference between the largest RSL and the smallest RSL is also within 12 dB at the same location for the O2D and O2DC scenario, while the difference for the O2O and R2R scenario limits within 5 dB. It suggests that a dedicated antenna radiating pattern pointing to the TX is important for the O2D and O2DC scenarios, which can provide more than 10 dB gain. The mean delay and RMS delay spread turn out to be stable for the O2O and R2R scenario, which means the existence of few reflections from surrounds. The mean delay and RMS delay spread for the O2D and O2DC scenario is large when the TX-RX distance is more than 15m, which shows that a lot of reflections from surrounds are incident at the receiver side. These information can provide good guideline for the placement of the future radio system.

ACKNOWLEDGMENT

The authors are thankful for the support of the European Commission through the Roll2Rail project, one of the lighthouse projects of Shift2Rail within the Horizon 2020 program. The Roll2Rail project has received funding from the European Unions Horizon 2020 research and innovation program under Grant Agreement no. 636032. Also the authors want to express their acknowledgements to ALSTOM for the support during the trials.

REFERENCES

- [1] Shift2rail Multi Annual Plan, Final version, November 2015
- [2] J. Goikoetxea, Roadmap towards the wireless virtual coupling of trains, Nets4train workshop, San Sebastian, June 2016, Springer
- [3] European Project Smiler (Short Range Microwave Links: Present and Future), FP2-DRIVE 1
- [4] S. Salous, COST IC1004 White Paper on Channel Measurements and Modeling for 5G Networks in the Frequency Bands above 6 GHz
- [5] B. Ai, K. Guan, M. Rupp, T. Küner, X. Cheng, X-F. Yin, Q. Wang, G-Y. Ma, Y. Li, L. Xiong, and J-W. Ding, Future Railway Services-Oriented Mobile Communications Network, Special issue On Future Railway Communications, IEEE Communication magazine, October 2015, pp78-85, 2015.
- [6] <http://www.roll2rail.eu/>
- [7] K. Nakamura, K. Kawasaki, N. Iwasawa, D. Yamaguchi, Application of the 90 GHz Band Millimeter-Wave in the Railway, WCRR, 2016.
- [8] T. Ganesh, K. Pahlavan, Statistics of short time and spatial variations measured in wideband indoor radio channels, *IEE proceedings-H*, Vol.140, No.4, Aug, 1993.
- [9] A. F. Molisch, *Wireless Communications*. John Wiley & Sons, 2007.
- [10] Matthias Patzold, *Mobile Radio Channels*. John Wiley & Sons, second edition, 2011.